Estimating discharge in rivers through the combined use of dimensionless isovels and point velocity measurements

G. Farina, S. Alvisi and M. Franchini

ABSTRACT

This paper presents a procedure for estimating discharge in a river cross-section based on the combined use of dimensionless isovels and point velocity measurements. Specifically, taking the Biot–Savart law on the magnetic field induced by an electric current in a wire as their basis as already done by other researchers, the authors propose a new formulation of the relationship characterizing the effect of the wetted perimeter on the range of velocities in a cross-section in order to take explicit account of roughness, expressed by means of Manning's coefficient. Once appropriately nondimensionalized, the isoeffect contours can be read as dimensionless isovels. Assuming *in situ* velocity measurements are available, discharge at a cross-section can be computed using two different methods. The proposed procedure was applied to six case studies characterized by river cross-sections which differed greatly from one another. The results show that the two methods proposed for estimating discharge lead to equivalent outcomes, and in all the cases the procedure as a whole enables a sufficiently accurate estimation of discharge, even when it is based on a limited number of velocity measurements or on the measurement of maximum surface-water velocity alone.

Key words | discharge, isovel, measurement, surface-water velocity

G. Farina (corresponding author)
S. Alvisi
M. Franchini
Engineering Department,
University of Ferrara,
Via Saragat 1,
44122 Ferrara,
Italy
E-mail: *frngli@unife.it*

INTRODUCTION

The discharge of a river is by definition the volume of water that flows through a generic channel cross-section in a given unit of time. Its expression is given by:

$$Q = \int_A v \cdot n \, dA \tag{1}$$

where v and n represent, respectively, the velocity vector and the unit vector, the former having the same direction as the local flow of the water, the latter being normal to the surface A at the point considered. Equation (1) thus shows how discharge measurements are based on stream velocity measurements within the cross-section, whose bathymetry is assumed to be known.

In this context, the most common method for measuring discharge is the velocity-area method, which entails sampling the stream velocity in points located at different depths along a sufficient number of verticals distributed within the flow area. The velocity measurements are usually performed using a propeller-type current meter. This device is capable of deriving the stream velocity at the point of immersion based on the number of revolutions of the propeller over a pre-established interval of time; various types of deployments are possible (measurement by wading, or from a bridge, cableway or boat), depending on the dimensions of the cross-section.

The sampling verticals, appropriately spaced to provide an adequate representation of the variations in velocity over the extent of the cross-section, form an ideal surface that should be – insofar as is possible – flat, vertical and orthogonal to the general direction of streamflow. At the same time, the bathymetric profile of the cross-section is schematically represented by connecting the bottom points of the

doi: 10.2166/nh.2017.029

different verticals, and the flow area (A) is identified as the area between the cross-section profile and the free surface of the stream. This area is discretized into an adequate number of segments, for each of which the respective discharge is determined as the product of the corresponding area and respective mean velocity; the latter is obtained by means of point velocity measurements. Finally, the total discharge is calculated by approximating the integral of Equation (1) as the sum of the discharges of the individual segments. Although the velocity-area technique is generally recognized, one of the most accurate methods of discharge estimation (Herschy 2009), it is laborious and time-consuming, entails a considerable commitment of equipment/personnel and provides lower accuracy in proximity to the river bed due to the presence of vegetation; moreover, the strong currents that typically occur during exceptional flood events may expose operators to hazards or even make it impossible to take proper flow velocity measurements.

In order to make the sampling process faster and easier, measurements of an episodic type have been automated with the stationary or moving-boat technique, which involves the use of an Acoustic Doppler Current Profiler (ADCP) mounted on a boat or tethered from a bridge or river bank. This ultrasonic sensor emits acoustic pulses to determine, by virtue of the Doppler effect, the two-dimensional stream velocity and depth of the river bed. Measurements taken using ADCPs are thus extremely detailed; however, they are also costly, given the advanced instrumentation employed. What is more, the utility of ADCPs are limited, in particular, when (a) velocities are extremely high and the channel cross-sections become impassable to the equipped moving boats, (b) excessive shear creates turbulent conditions, (c) high concentrations of sediment cause difficult bottom detection due to sound wave attenuation and problems in depth measurement, and (d) in gin-clear waters where scatters are non-existent.

Since the time and cost involved in measuring discharge are proportional to the number of the velocity measurements to be performed, numerous studies have aimed to define criteria for estimating discharge on the basis of an extremely reduced number of sampled velocities; this would also make it possible to overcome the difficulties inherent in collecting hydrometric information during flood events.

A new method to determine the depth where the stream velocity is equal to the mean value along each vertical was derived from the experiences of Rouse (1950), by relying on the theory of turbulent motion. This approach (One-Point Method, UNI EN ISO 748 2008) (Rantz 1982; Moisello 1998) is easy to apply and makes it possible to derive the mean velocity along a number of verticals based solely on knowledge of the point velocity measured at a distance equal to 60% of the water depth below the free surface, in order to directly apply the velocity-area method. Unfortunately, the corresponding logarithmic velocity distribution model fits the real situation rather poorly and the velocity measurement may be inaccurate, so this approach is relied on only when it is absolutely necessary to save time.

A valid alternative for estimating discharge is the entropy concept: it is founded on the principle of entropy maximization (Jaynes 1957) and has been applied by Chiu (1987, 1988) to reconstruct the velocity distribution in probability space in a channel cross-section. Chiu identified a linear relationship, function of a parameter M, between the mean velocity $\bar{U}$ and the maximum velocity $u_{\max}$ in a river cross-section (Chiu 1988, 1991; Xia 1997), i.e., $\bar{U} = f(u_{\max}, M)$. In practical terms, based solely on a measurement of the cross-sectional maximum velocity $u_{\max}$ (easily determinable, as it generally manifests itself in the upper-middle portion of the flow area, which remains readily accessible for sampling even during major floods (Chiu & Murray 1992; Chiu & Abidin Said 1995; Moramarco *et al.* 2004; Corato *et al.* 2012), it is possible to arrive at an estimate of the mean velocity $\bar{U}$ and then, by multiplying the latter by the cross-sectional flow area, at an estimate of discharge.

However, the parameter M must first be estimated to convert the maximum observed velocity $u_{\max}$ into the cross-sectional mean velocity $\bar{U}$; this dimensionless parameter represents a typical constant of a generic cross-section of a channel or river (Chiu 1988, 1989; Chiu & Murray 1992; Chiu & Abidin Said 1995; Moramarco & Singh 2010) and is generally estimated by linear regression performed on pairs of values $u_{\max} - \bar{U}$, which are in turn obtained by means of the velocity-area method; it thus requires numerous *in situ* velocity measurements taken during low-flow and flood events. While Chiu & Tung (2002) suggested determining M through velocity sampling

at several depths along the y-axis (i.e., the vertical axis where the maximum velocity occurs), a recently proposed procedure (Farina *et al.* 2014) enables the parameter M to be estimated on the basis of the maximum surface velocity measurement alone. Essentially, using this procedure, it is possible (based solely on the measurement of maximum surface velocity) both to estimate the parameter M independently of the velocity-area method and calculate u_{max} as a function of the only sampled velocity. The mean velocity can then be estimated and multiplied by the cross-sectional flow area to obtain the discharge. It is worth noting that nowadays the aforesaid maximum surface velocity can be easily measured using simple and practical 'non-contact' radar sensors based on the Doppler effect (Costa *et al.* 2000, 2006; Melcher *et al.* 2002; Cheng *et al.* 2004; Fulton & Ostrowski 2008); an alternative approach is based on particle image velocimetry (Adrian 1991) with a fixed camera which can be installed on a roof (Creutin *et al.* 2003), on a bridge (Tauro *et al.* 2016), on a telescopic rod (Jodeau *et al.* 2008) or on a tripod (Tauro *et al.* 2012) and even remotely piloted aircraft systems (Tauro *et al.* 2015). Moreover, few studies have demonstrated that it is possible to measure river hydraulic data, including the surface velocity, entirely from satellites in order to develop general approaches to estimate river discharge from space (Bjerklie *et al.* 2003).

Recently, other authors have also attempted to estimate discharge in a river cross-section while limiting the sampling step to a single point velocity measurement. The approach developed by Maghrebi (2003) draws its inspiration from the Biot–Savart law (Hayt 1981), which can be used to calculate the intensity of a magnetic field generated at a point in space by an infinitely long wire carrying a stationary and steady current. The authors applied this law to the field of hydraulics to quantify the effect on velocity at a generic point in a channel cross-section, as produced by a generic portion among those into which the wetted perimeter is divided. This effect is proportional to the roughness of that portion of the wetted perimeter, according to a constant c and the distance separating it from the point considered. The approach described enables the pattern of isoeffect contours, duly nondimensionalized, to be represented based on the geometry of the bathymetric profile and hydraulic characteristics of the river bed. These contours can be read as dimensionless isovels (normalized to the cross-sectional mean velocity). This means that it is sufficient to measure the velocity at any point in order to be able to estimate, based on the ratio between that measurement and the dimensionless velocity at that point, the cross-sectional mean velocity and hence the discharge, where the flow area is known. The proposed approach was applied mainly to synthetic case studies and considering just one velocity measurement to estimate the cross-sectional mean velocity (Maghrebi 2003; Maghrebi & Rahimpour 2005; Rahimpour & Maghrebi 2006).

Unfortunately, in Maghrebi's formulation (2003) an ambiguous point remains, namely, the manner in which the roughness of a single bed portion influences velocity at a generic point in the cross-section. In fact, although in Maghrebi (2006) it is stated that 'c is a constant related to the boundary roughness … for rougher boundaries c takes smaller values', Rahimpour & Maghrebi (2006) write, in seeming contradiction, that 'c is a constant which is related to the boundary roughness (for rougher boundaries c takes larger values)'.

In light of the above, we propose a different approach for tracing isovels. Similarly to Maghrebi (2006), the proposed approach takes the Biot–Savart law as a starting point, but differently to Maghrebi (2006), it relies on Manning's roughness coefficient of the wetted perimeter and a different law to quantify the effect on velocity at a generic point in a channel cross-section, as better shown in the subsequent sections. Once we have reconstructed the isovel pattern associated with a particular roughness configuration, we can then calculate discharge on the basis of one or more (differently to Maghrebi (2006)) sampled velocity measurements performed within the flow area.

Below, we present a summary of the basic concepts of the Biot–Savart law, as they represent the theoretical basis of this study and a tool for the reconstruction of isovels in a generic river cross-section. We then show how these isovels can be drawn depending on the roughness configuration and how they can be used to estimate discharge on the basis of at least one velocity measurement. The proposed procedure is applied in several real case studies: cross-sections at the Ponte Nuovo and Santa Lucia gauging stations along the Tiber River (Italy), the Pontelagoscuro gauging station along the Po River (Italy), as

well as some cross-sections of the Ohio, Allegheny and Monongahela Rivers in the USA. After describing the results for these cross-sections, we present some final considerations.

THE BIOT–SAVART LAW AND ITS EXTENSION TO HYDRAULICS

In magnetostatics it has been amply demonstrated that a current – i.e., charges moving at a constant velocity in a metal conductor – is capable of generating a magnetic field in the surrounding space. In the specific case of a straight wire carrying a current I, the lines of force of the generated magnetic field $\mathbf{H}$ remain circular and concentric (the common centre is the wire the current is passing through). It follows that at every point in space, the magnetic field vector $\mathbf{H}$ lies in a plane that is orthogonal to the current and tangent to a circumference whose centre is the wire; the direction of the vector will depend on the direction of the electric current I and can be simply derived by using the 'right-hand rule'. As far as the intensity of the magnetic field is concerned, it is easy to imagine that as the distance from the wire increases, the field will be progressively weaker, while it will become stronger as the current I increases. If we consider a curvilinear current-carrying wire, having a length L and a current I, as represented in Figure 1, an elemental segment $d\mathbf{l}$ of the wire, oriented according to the direction of the current, constitutes an elemental source which provides an elemental contribution to a magnetic field $d\mathbf{H}$ at any point O in space. The direction of the magnetic field $d\mathbf{H}$ (z-direction) is orthogonal to the plane formed by the vector $d\mathbf{l}$ and the unit vector $\mathbf{a}_R$, which goes from the source point to the field point (the xy-plane of the sheet). Its direction can be deduced using the right-hand rule (in this case the vector is directed toward the reader, see Figure 1), whereas its intensity is inversely proportional to the square of the distance r of the field point from the source point according to the following expression (Biot & Savart 1820; Hayt 1981):

$$d\mathbf{H} = \frac{1}{4\pi}\frac{Id\mathbf{1}\times\mathbf{a}_R}{r^2} \tag{2}$$

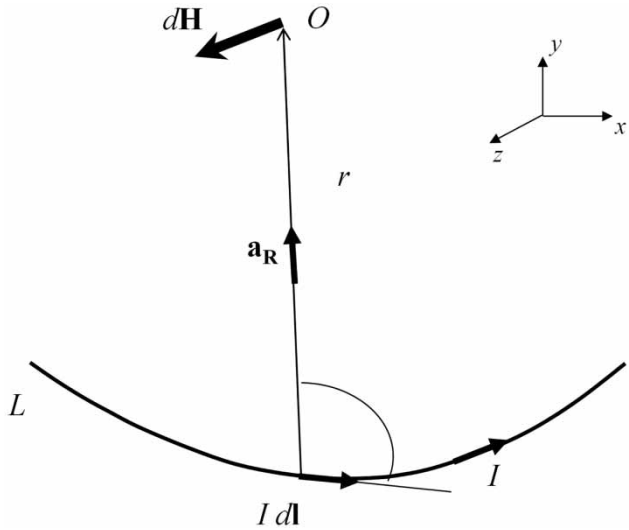

Figure 1 | Contribution to a magnetic field $d\mathbf{H}$ generated by an elemental segment $d\mathbf{l}$ of a curvilinear current-carrying wire having a length L and carrying a current I.

The field $\mathbf{H}$ generated at the point O by the entire current-carrying wire is determined by integrating Equation (2) along the curve of length L (Halliday & Resnick 1990):

$$\mathbf{H} = \int_L d\mathbf{H} = \int_L \frac{1}{4\pi}\frac{Id\mathbf{1}\times\mathbf{a}_R}{r^2} \tag{3}$$

By applying this concept to a hypothetical infinite cross-section where each point is infinitely far away from the contour, the water would remain undisturbed and characterized by a uniform velocity distribution; however, as the field of motion is confined within a contour, the stream in reality encounters resistance during its movement, since the particles close to the contour, which are stationary or exhibit a no-slip condition (the wetted perimeter is, in fact, made to coincide with the isovel having a value of zero), slow down the adjacent ones. This resistant effect is propagated from the contour to the middle, with an impact on the entire stream. In reality, therefore, the velocity distribution at a river cross-section is not uniform and the velocity tends to decrease near the river bed, more or less intensely depending on its geometry and hydraulic characteristics. It is, in fact, known that the rougher the contour, the higher will be the resistance it provides to the water. In light of these considerations, the cross-section contour, i.e., the wetted perimeter (likened to a wire), characterized by a

certain distribution of roughness, can be considered to influence the pattern of flow velocities in a given cross-section, just as the current-carrying wire is the source of a magnetic field in the surrounding space, as previously described. This analogy between magnetostatics and hydraulics enables us to calculate the effect generated by the wetted perimeter on velocity at a generic point in the cross-section miming the Biot–Savart law.

Let us consider a river cross-section in which the wetted perimeter is divided into elemental segments having a length $d\mathbf{s}$, each segment representing a vector oriented from the right bank to the left bank, as illustrated in Figure 2. The elemental effect $d\mathbf{e}_{u_o}$ produced by a generic element $d\mathbf{s}$ of the wetted perimeter on the velocity u at a point O within the cross-section can be expressed as:

$$d\mathbf{e}_{u_o} = d\mathbf{s} \times \mathbf{f}(\mathbf{r}, n) \tag{4}$$

where n is the roughness of the element $d\mathbf{s}$ and $\mathbf{r}$ represents the position vector of the point O.

While in the formulation proposed by Maghrebi the roughness of the wetted perimeter is represented by a multiplicative factor c which is outside the vector product $d\mathbf{s} \times \mathbf{f}(\mathbf{r})$, in this study roughness, described by means of the Manning coefficient, n, becomes a variable inside the vector product; specifically, the function $\mathbf{f}$ is dependent on both roughness and the distance $\mathbf{r}$.

As in the case of Equation (3), used to calculate the magnetic field $\mathbf{H}$ generated at the point O by the entire current-carrying wire, the total effect $\mathbf{e}_{u_o}$ generated by the entire wetted perimeter on the velocity u at a point O within the cross-section is calculated by integrating Equation (4) along the extent P of the boundary as shown below:

$$\mathbf{e}_{u_o} = \int_P d\mathbf{e}_{u_o} = \int_P d\mathbf{s} \times \mathbf{f}(\mathbf{r}, n) \tag{5}$$

It is known that the vector product $d\mathbf{s} \times \mathbf{f}(\mathbf{r}, n)$ is a vector normal to the plane xy formed by the vectors $d\mathbf{s}$ and $\mathbf{r}$ (coinciding with the plane of the sheet), and having a modulus equal to $ds \cdot f(r, n) \cdot \sin\alpha$, where α is the angle comprised between the vector position $\mathbf{r}$ and the vector element $d\mathbf{s}$; it follows that the vector $\mathbf{e}_{u_o}$ is also normal to the plane xy, and hence directed according to the z-axis, in particular toward the reader (Figure 2). Since the angle θ comprised between the vector position $\mathbf{r}$ and the vector normal to the element $d\mathbf{s}$ is complementary to α, we may deduce that $\cos\theta = \sin\alpha$; therefore, from Equation (5) we derive the *modulus* of the total effect e_{u_o} produced by the wetted perimeter on the velocity u at a point O:

$$e_{u_o} = \int_P f(r, n) \cdot \cos\theta \cdot ds \tag{6}$$

The function $f(r, n)$ of Equation (6) can be assumed – based on the Chen power-law of velocity distribution (Chen 1991a) derived from a partial differential equation describing the steady uniform turbulent flow of a fluid in a pipe or an open channel – to be equal to the following expression:

$$f(r, n) = c \cdot u_* \cdot \left(\frac{r}{k_s}\right)^{1/m} \tag{7}$$

where c is a coefficient that varies with the global Reynolds number for hydraulically smooth flows or with global relative roughness for fully rough flow, $u_* = \sqrt{\tau_0/\rho}$ is the friction velocity in which τ_0 is the boundary shear stress and ρ is the mass density of fluid. The exponent m usually ranges between 4 and 12 depending on the intensity of the turbulence (Yen 2002). A value of 7 agrees well with the results of a large number of experimental measurements of turbulent velocity profiles (Chen 1991b; Wright & Parker 2004) even though the sensitivity of the velocity profile to the variation of power m is not high (Chen 1991b). k_s is the

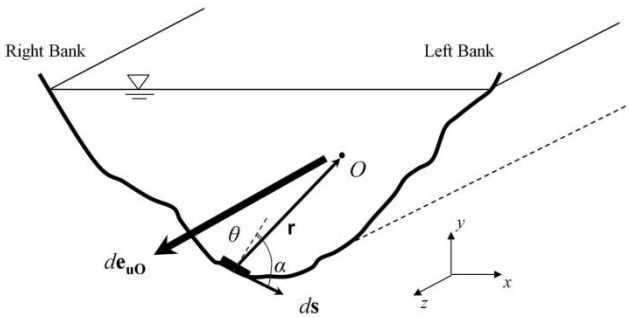

Figure 2 | Elemental effect $d\mathbf{e}_{uo}$ on the velocity u at a point O within the cross-section produced by a generic element $d\mathbf{s}$ of the wetted perimeter.

equivalent Nikuradse sand roughness height; experimental trials conducted by Strickler (1923) have shown that the roughness height k_s, in turbulent conditions, can be expressed as a function of the Manning coefficient n as follows:

$$k_s = \left(\frac{n}{0.0342}\right)^6 \tag{8}$$

Equation (6), rewritten after substituting Equations (7) and (8), enables the dependence of the total effect e_{u_o} on the Manning coefficient n and the distance r to be directly expressed as follows:

$$e_{u_o} = \int_P c \cdot u_* \cdot \left(\frac{r}{(n/0.0342)^6}\right)^{1/m} \cdot \cos\theta \cdot ds \tag{9}$$

Considering that Equation (9) is valid for any point O inside the flow area A, the total mean cross-sectional effect E_u on velocity generated by the wetted perimeter is given by:

$$E_u = \frac{1}{A} \cdot \int_A e_{u_o} dA = \\ = \frac{1}{A} \cdot \int_A \left(\int_P c \cdot u_* \cdot \left(\frac{r}{(n/0.0342)^6}\right)^{1/m} \cdot \cos\theta \cdot ds \right) dA \tag{10}$$

The normalized effect on velocity generated by the wetted perimeter at the generic point O is calculated by means of the ratio between e_{u_o} and E_u, provided by Equations (9) and (10), respectively; with any distribution of roughness, non-uniform or constant, assuming a constant friction velocity along the wetted perimeter, it can be expressed as:

$$\eta_o = \frac{e_{u_o}}{E_u} \\ = \frac{\int_P \left(r/(n/0.0342)^6\right)^{1/m} \cdot \cos\theta \cdot ds}{1/A \cdot \int_A \left(\int_P \left(r/(n/0.0342)^6\right)^{1/m} \cdot \cos\theta \cdot ds\right) dA} \tag{11}$$

It is worth noting that the assumption of constant friction velocity is correct for wide open channels which is usually the case for natural rivers (Chow 1959; Krishnappan & Lau 1986; Nezu & Nakagawa 1993; Rodi 1993; Maghrebi 2006). For narrower cross-sections, the assumption may be approximate.

Equation (11) enables the pattern of the 'isoeffect' contours, duly nondimensionalized, to be represented taking into account the geometry of the bathymetric profile and the hydraulic roughness characteristics of the river bed according to Manning's coefficient.

If we assume that the stream velocity u_O is proportional, at any point O, to the total effect e_{u_o} produced by the wetted perimeter on that velocity according to a constant k:

$$u_O = k \cdot e_{u_o} \tag{12}$$

by continuity, the same law of direct proportionality applies between the cross-sectional mean velocity $\bar{U}$ and the total mean cross-sectional effect E_u generated on velocity by the wetted perimeter, i.e.:

$$\bar{U} = k \cdot E_u \tag{13}$$

therefore, dividing Equations (12) and (13) member by member it follows that:

$$\frac{u_O}{\bar{U}} = \frac{e_{u_o}}{E_u} = \eta_O \tag{14}$$

Thanks to the latter equation, the dimensionless isoeffect contours can be simultaneously read as dimensionless isovels, normalized relative to the cross-sectional mean velocity.

The knowledge of the dimensionless isovels implies that it is sufficient to have the velocity measurement at any point O in order to estimate the cross-sectional mean velocity based on the ratio between the measurement u_O and the corresponding dimensionless velocity η_O at that point as follows:

$$\bar{U} = \frac{u_O}{\eta_O} \tag{15}$$

It is important to stress that, in a real cross-section, the application of Equation (15) at different points within the flow area is expected to lead to different estimates of the cross-sectional mean velocity, since the proposed method is by its very nature approximate; if it were not so, the estimated cross-sectional mean velocity would be the same at all points and there would be a perfect coincidence between the isovels reconstructed with this method and the actually observed ones. Precisely for this reason, the estimation of the cross-sectional mean velocity can only come from a duly computed average of the values of $\bar{U}$ obtained at each selected point, and based, therefore, on various sampled velocity measurements.

The following two sections give (a) a more in-depth analysis of the dimensionless isovel pattern reconstruction procedure and its sensitivity both to the section geometry and river bed roughness distribution and (b) a description of two formulations to estimate the cross-sectional mean velocity starting from several sampled velocity measurements.

However, before concluding this section, given the very nature of the proposed procedure to define the isovels in a cross-section, it is worth highlighting that the reach around the cross-section selected should comply as far as possible with the following requirements:

1. the channel at the measuring site should be straight and of uniform cross-section in order to minimize abnormal velocity distribution which could not be caught by the isovels reconstructed through the proposed method;
2. flow directions for all the sampled velocity points within the flow area should be parallel to each other and at right angles to the measurement section;
3. the section should be sited away from pumps, sluices, outfalls, converging or diverging flow.

Incidentally, all these requirements coincide with those indicated for selecting appropriate cross-sections for discharge measurements through the velocity-area method, for instance UNI EN ISO 748 (2008).

Finally, we would like to highlight that the bed slope and any cross-section geometry variation could affect the value/s of the punctual velocity used in the second phase of the method to make the isovel pattern estimated in the first phase dimensional. Thus, both of them are implicitly taken into account in the method.

SENSITIVITY ANALYSIS AND REPRESENTATIVENESS OF THE DIMENSIONLESS ISOVEL PATTERN RECONSTRUCTION PROCEDURE

Figure 3 shows the isovels, drawn following the procedure described in the previous section, in the case of a rectangular cross-section where the ratio between B (width) and H (depth) varies from 0.25 to 10.0 and the Manning coefficient is constant along the wetted perimeter and equal to $0.02\ \mathrm{m}^{-1/3}\ \mathrm{s}$. It is worth noting that the maximum velocity is correctly below the water surface when the ratio B/H is small while it moves towards the water surface as the ratio B/H increases, consistently with the cross-sectional velocity pattern generally reported in the scientific literature for narrow and wide rectangular cross-sections (e.g., Marchi & Rubatta 1981; Chiu & Chiou 1986). Moreover, isovels are symmetric and the maximum velocity occurs in the centreline of the cross-section.

Figure 4 shows the effect of the Manning coefficient along the cross-section perimeter on the isovels. It can be observed that the proposed procedure leads to realistic isovel patterns not only in the case of uniform roughness along the wetted perimeter (Figure 4(a)) but also in the case of composite roughness (Figure 4(b) and 4(c)). In particular, the proposed procedure allows non-symmetric isovels to be properly represented in the case of non-symmetric composite roughness (Figure 4(b)), where the maximum velocity has deviated from the centreline of the cross-section; furthermore, it is shown that the maximum velocity has deviated away from the more roughened surfaces, lateral surface (Figure 4(b)) and bottom surface (Figure 4(b) and 4(c) vs 4(a)).

It is interesting to observe that when the Manning roughness coefficient is assumed uniform along the wetted perimeter, independently of its value, the pattern of the non-dimensional isovels depends only on geometry of the bathymetric profile. In fact, Equation (11) mathematically reduces to:

$$\eta_O = \frac{e_{u_O}}{E_u} = \frac{\int_P (r)^{1/m} \cdot \cos\theta \cdot ds}{1/A \cdot \int_A \left(\int_P (r)^{1/m} \cdot \cos\theta \cdot ds \right) dA} \tag{16}$$

According to the method, this means that a uniform roughness only affects the actual value of the velocities in the cross-section but not their relative distribution. This can

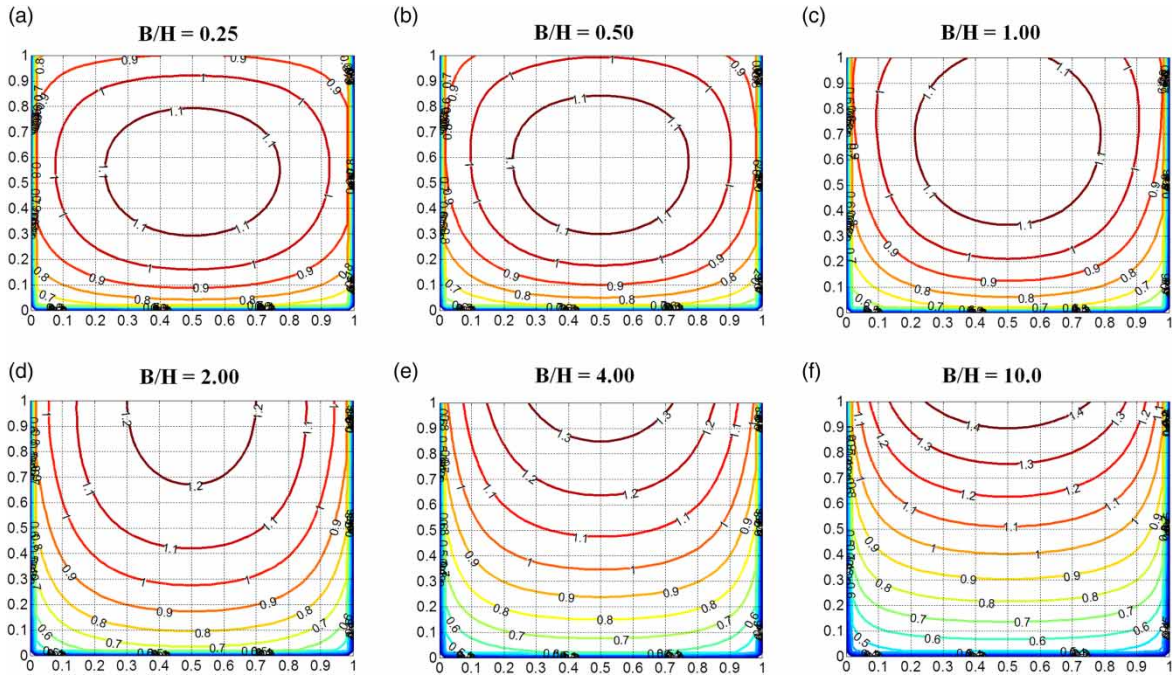

Figure 3 | Dimensionless isovel pattern in a rectangular channel cross-section with different B (weight)/H (height) ratios.

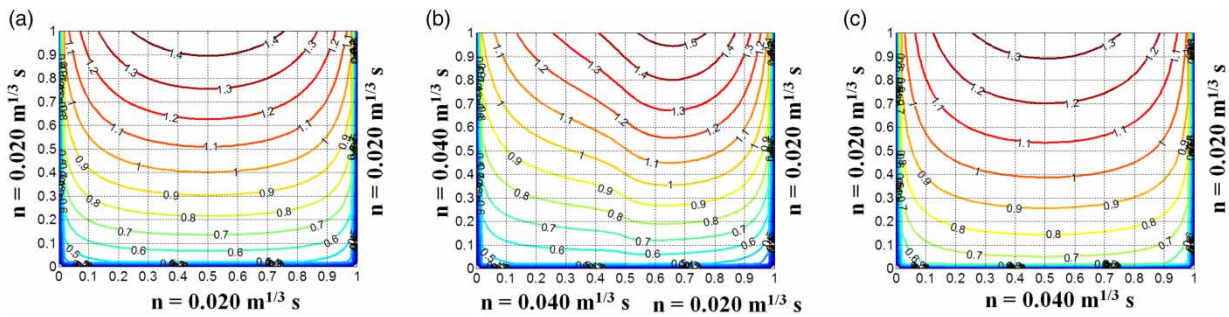

Figure 4 | Effect of uniform roughness (a) and composite roughness (b) and (c) on the isovel pattern.

be acceptable in the case where the turbulent regime is fully developed.

While previous considerations are of qualitative type, in order to validate the representativeness of the isovels reproduced by the proposed model, a comparison with the velocity profiles observed in two gauge stations located along two natural channels was also performed.

First, making reference to the work by Yamaguchi & Niizato (1994) on the Unon river, the application of the proposed method was examined to obtain the surface velocities and compare the predicted results with the measurement data. The bed cover being composed of almost uniform roughness, except in a limited area of the river section close to the banks where the roughness elements are larger (Lee *et al.* 2002), we assumed a uniform distribution of roughness along the entire wetted perimeter; therefore, we reconstructed the isovel pattern based only on the shape of the cross-section by means of Equation (16) (Figure 5(b)).

In Figure 5(a), the predicted dimensionless water surface velocity is plotted against the measured surface velocity obtained using X-band radar technique (see Yamaguchi & Niizato 1994), in turn normalized through the mean velocity observed during the event; on the whole, a good agreement between the predicted and the measured water surface

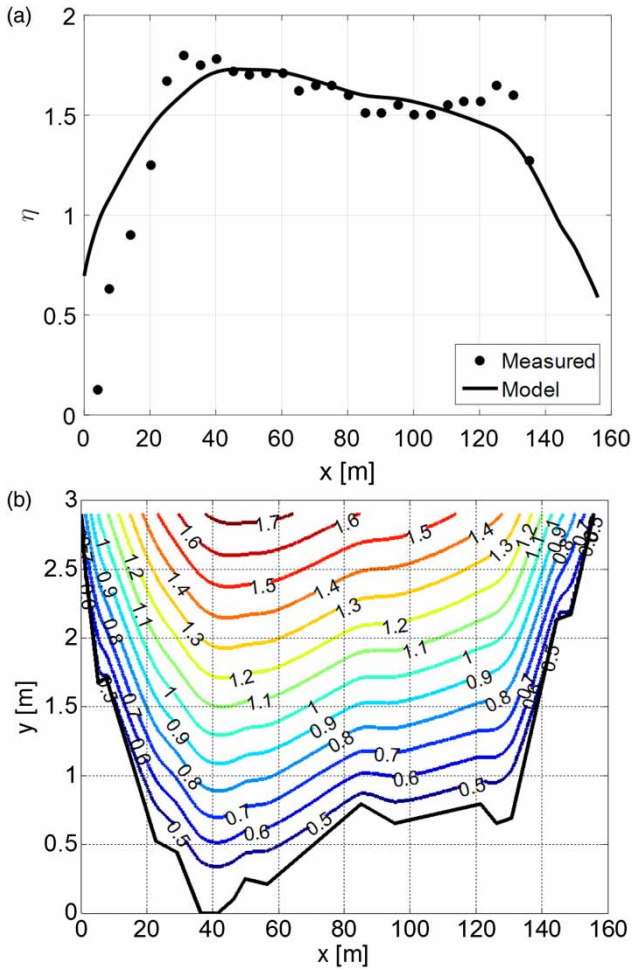

Figure 5 | (a) Predicted dimensionless water surface velocities (proposed method) against measured values, (b) predicted isovel pattern in the Unon river. Manning roughness coefficient is assumed constant along the wetted perimeter.

velocity can be observed, except for some deviations close to the banks where the predicted results are lower than the measured data, probably due to the ignorance of bed roughness near the boundary (see also Maghrebi 2006).

Second, the Pontelagoscuro gauging station on the Po River was considered (see the section 'Case studies' for further details), where measurements of discharge based on the mean-section method (UNI EN ISO 748 2008) are available. The highest flood event during the years 1984–1992 was selected: it occurred on October 16, 1987 and it was characterized by discharge equal to 5,026 m^3/s. For this event, the current-meter velocity measurements along 16 verticals were considered. Since the discharge was known (computed with the mean-section method), the average velocity $\bar{U}$ was derived as well as the ratios 'measured point velocity/average velocity', $u/\bar{U}$, in all the measuring points. These values were compared with the corresponding values which characterized the non-dimensional isovel pattern produced by the proposed method, shown in Figure 6(b), still assuming a uniform roughness coefficient along the wetted perimeter (as no detailed information is available on this aspect) and thus reference to Equation (16) was made.

Figure 6(c) reproduces a comparison between the predicted and observed non-dimensional velocities along a selected vertical (indicated by a dashed line in Figure 6(a) and 6(b)) with respect to the ratio y/D where y is the distance from the bottom (where the generic velocity measurement is performed) and D is the total depth at the vertical considered. It is shown that the largest deviation is at the surface (y/D near to 1) which corresponds to a relative error equal to 22.5% (overestimate) which, however, may also be related to a certain error of the velocity measurement. The relative error reaches its minimum value equal to 1.4% at about half of the depth D (y/D near to 0.4) where the predicted and observed non-dimensional velocities almost coincide. In any case, the mean absolute percentage error is about 14%, thus confirming a good representativeness of the actual vertical velocity profile. Similar results are obtained along the other verticals with an increasing error near the banks.

Figure 6(a) reproduces a comparison between the observed mean non-dimensional velocities along all the 16 verticals and those produced by the proposed model. In this case as well, a good representativeness is observed, even though some discrepancies occur near the banks. This can be due to the effect of boundary eddies not represented by the proposed model and inaccurate evaluation of the roughness coefficient along the wetted perimeter.

Overall, these results confirm the validity of the method proposed for representing the water profiles in a cross-section and, in particular, the average value of the velocity, thus forming a reliable tool for the estimation of the discharge as shown in the section 'Analysis and discussion of the results'.

ESTIMATING DISCHARGE

On the basis of the issues discussed above, it is possible to formulate the following method for estimating discharge in a generic channel cross-section. The first step is to

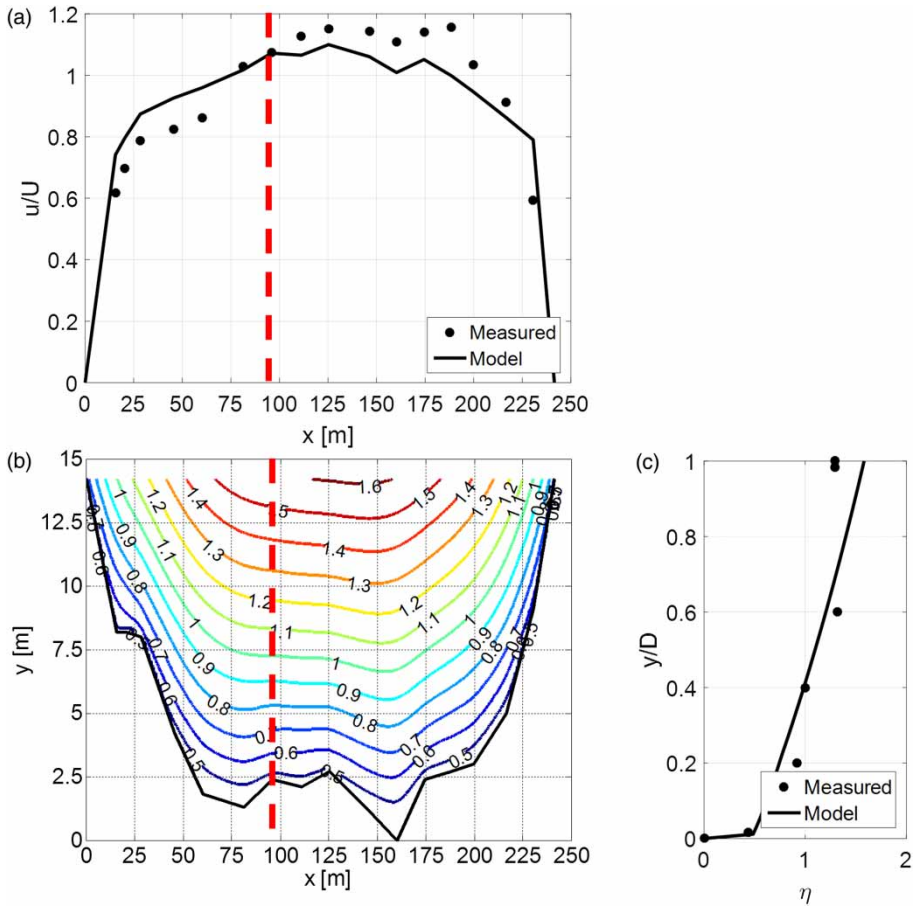

Figure 6 | (a) Predicted depth-averaged dimensionless velocities (proposed method) against measured values, (b) predicted isovel pattern, (c) comparison of the dimensionless measured data along a selected vertical with the normalized vertical profile produced by the proposed model at the Pontelagoscuro gauging station along the Po river. Manning roughness coefficient is assumed constant along the wetted perimeter.

reconstruct the isovel pattern based on the shape of the cross-section and roughness configuration along the wetted perimeter by means of Equations (11) or (16) if the roughness distribution is uniform. Once this pattern has been constructed, assuming we have at our disposal n_{meas} sampled velocity measurements within the flow area, each measurement will produce a different estimate of the cross-sectional mean velocity, due to the approximation of the method; the cross-sectional mean velocity, and thus discharge, which takes into account all velocity measurements, can be determined in two different ways.

In the first case, after we have calculated the cross-sectional mean velocity $\bar{U}_i$ (with $i = 1,2,\ldots n_{meas}$) according to Equation (15) and on the basis of each of the n_{meas} sampled velocity measurements, the actual cross-sectional mean velocity will be given by the mean of the values of $\bar{U}_i$ thus estimated; therefore, the flow area being known, the discharge Q_{sim1} will be:

$$Q_{sim1} = \bar{U}A = \left(\frac{1}{n_{meas}}\sum_{i=1}^{n_{meas}}\frac{u_i}{\eta_i}\right)A \tag{17}$$

Given that, as already noted, the individual point velocity measurement enables us to estimate the cross-sectional mean velocity and thus discharge, in reality, Q_{sim1} can also be read as the arithmetic mean of discharge values $Q_i = (u_i/\eta_i)A$ (with $i = 1,2,\ldots n_{meas}$).

In the second case, we consider the n_{meas} point measurements u_i ($i = 1,2,\ldots n_{meas}$) together and the corresponding objective function given by the sum of the squares of the deviations between the reproduced dimensionless velocities η_i and the potentially observed ones $u_i/\bar{U}$ at the n_{meas}

measurement points as follows:

$$OF = \sum_{i=1}^{n_{meas}} \left(\frac{u_i}{\bar{U}} - \eta_i \right)^2 \tag{18}$$

Assuming the optimal value of $\bar{U}$ to be the one that minimizes the above objective function OF, thus deriving OF with respect to $\bar{U}$ and setting the derivative equal to zero, the resulting discharge will be equal to:

$$Q_{sim2} = \bar{U}A = \frac{\sum_{i=1}^{n_{meas}} u_i^2}{\sum_{i=1}^{n_{meas}} u_i \cdot \eta_i} A \tag{19}$$

CASE STUDIES

The proposed procedure for estimating discharge was applied to six different case studies involving channel cross-sections at the Ponte Nuovo and Santa Lucia gauging stations (Tiber River), Pontelagoscuro gauging station (Po River), as well as some cross-sections of the Ohio, Allegheny and Monongahela Rivers in the USA.

Figure 7 shows the bathymetric survey data for the river cross-sections in question. As can be seen, the study sites are characterized by very wide rectangular/trapezoidal cross-sections. However, their cross-section dimensions vary and, in particular, the width ranges from a minimum of 35 m in the case of the Santa Lucia to a maximum of 380 m in the case of the Ohio River, whereas the height ranges from a minimum of 6 m to a maximum of 9 m for the same cross-sections.

The Ponte Nuovo, Santa Lucia and Pontelagoscuro gauging stations are equipped with a level gauge and the current-meter measurements were performed along different verticals and at different depths; in the remaining gauging stations, the velocity measurements were made by means of the moving-boat technique, i.e., using a small moving boat equipped with an ADCP.

It is common practice to make four or more 'good' transects (i.e., traversing the river cross-section with a boat) under relatively steady flow conditions and average them to get a reliable ADCP discharge measurement; indeed, the proposed method was applied to ADCP velocity data extracted from the computational grid of each transect in order to compare the simulated discharge with the observed one. In this paper, the results of a single transect are shown for the sake of brevity.

With regard to the ADCP approach, it is necessary to measure the velocity orthogonal to each of the numerous cells into which it is possible to divide the flow area generated by the vertical projection of the boat's course. In this respect, use of Winriver II software (RDI 2007) was made. Through this software the following information was

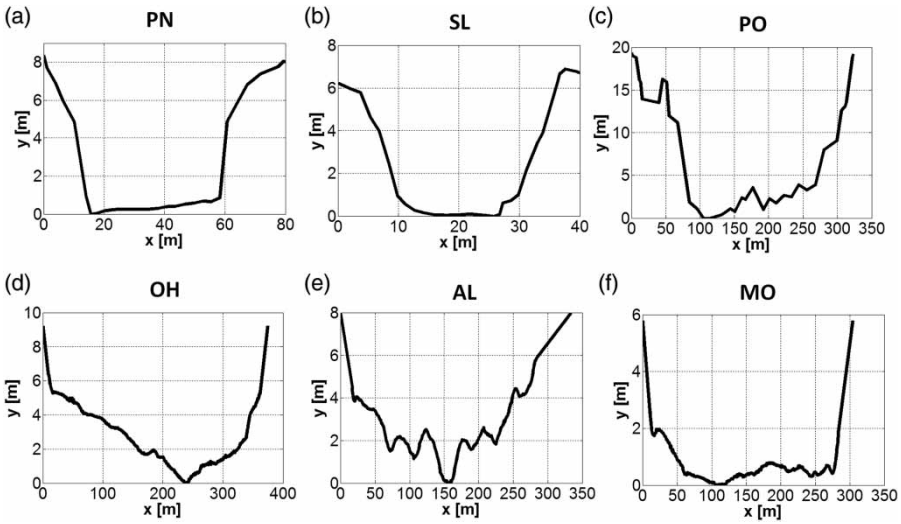

Figure 7 | Bathymetric surveys of analysed river sites: (a) Ponte Nuovo (PN), (b) Santa Lucia (SL), (c) Pontelagoscuro (PO), (d) Ohio (OH), (e) Allegheny (AL), (f) Monongahela (MO).

extracted. Given that the boat's course cannot be a perfectly straight line, the cross-section it ideally draws is not flat; as cross-section planarity is a fundamental assumption of the proposed method, in order to satisfy this condition it is necessary to have, for each individual cell, the projection of its area on a plane which is orthogonal to the average one of the stream and the component of velocity orthogonal to the generic cell in a direction parallel to the average one of the stream.

The velocity thus determined for an individual cell can then be compared with the measurement made with a single current meter. Despite the current-meter measurements and hydroacoustic measurements being based on completely different techniques and take different times for the velocity sampling, both methods get stream point velocity measurements along several verticals within the cross-section, which can be considered representative of each corresponding individual cell/subarea and can be used to estimate the discharge through the velocity-area method. In particular, the velocity measurements obtained with the ADCP system can be viewed as equivalent to those obtained with a series of current meters evenly spaced along a generic vertical lying in a flat cross-section.

As regards the events, the set of data relating to the Ponte Nuovo, Santa Lucia and Pontelagoscuro gauging stations embraces numerous flood events recorded in different periods of the year, while the available measurements for the Ohio, Allegheny and Monongahela river cross-sections refer to a single event. For each event, the set of sampling velocities across the entire hydrometric cross-section of each gauging station, from the surface to the bottom, will be hereafter indicated as S1.

We would like to stress that both with the ADCP technique and with a current meter the surface velocity cannot be measured, and in order to apply the proposed method we considered it equal to that closest to the water surface. This assumption was quite reasonable given that the observed vertical velocity profile in those sections was characterized by a rather constant velocity as approaching the water surface.

Table 1 shows the number of events N and ranges with respect to the main hydraulic characteristics, cross-sectional mean velocity $\bar{U}$, flow area A and discharge Q_{obs}. In particular, as already observed, the discharge Q_{obs} was calculated on the basis of the point velocity measurements using the Mean-Section Method (UNI EN ISO 748 2008) at Ponte Nuovo, Santa Lucia and Pontelagoscuro cross-sections where velocity measurements were performed using a current meter; while using the Winriver II software at the Ohio, Allegheny and Monongahela cross-sections equipped with an ADCP. The cross-sectional mean velocity $\bar{U}$ was obtained by dividing this discharge value by the flow area.

ANALYSIS AND DISCUSSION OF THE RESULTS

The numerical analyses were conducted in the following manner.

There being no available information about the state of the river bed at the cross-sections, a uniform distribution of roughness was assumed for each of them; the considerations and analyses that follow thus derive from isovel patterns reconstructed by means of Equation (16).

First, for each case study considered, the observed discharge Q_{obs} was compared with the discharges Q_{sim1} and

Table 1 | Interval of main quantities observed during N flood events at river gauging stations

Location	N	Period/Date	$\bar{U}$ [m/s]	A [m^2]	Q [m^3/s]
Ponte Nuovo	55	1982–2007	0.15–1.97	31.20–311.91	5.76–541.58
Santa Lucia	19	1990–2004	0.15–2.02	11.20–91.76	1.71–185.33
Pontelagoscuro	48	1984–1992	0.35–2.05	913.12–2,833.06	316.18–5,026.00
Ohio	1	27/03/2008	0.58	2,366.51	1,362.02
Allegheny	1	26/03/2008	0.79	1,577.86	1,248.00
Monongahela	1	20/05/2008	0.77	1,468.05	1,134.98

Q_{sim2} estimated by means of Equations (17) and (19), relying on all the n_{meas} sampled velocity measurements available for each event (set S1). This type of analysis allowed assessment of the reference accuracy of the discharge estimation method proposed.

Second, the discharge at each gauging station considered was estimated taking into account several subsets of point velocity measurements in order to determine how it would be possible to reduce the number of measurements and obtain acceptable discharge estimates at the same time.

First step

The discharges Q_{sim1} and Q_{sim2} (Equations (17) and (19)) obtained using all point velocity values u_i (with $i = 1,2 \ldots n_{meas}$, set S1) and the observed discharge Q_{obs} for the N events available were compared with each other for all the considered gauging stations, assuming a uniform distribution of roughness along the wetted perimeter.

On the basis of the N pairs of values $Q_{sim1} - Q_{obs}$ and $Q_{sim2} - Q_{obs}$, a measure of prediction accuracy of the proposed method was quantified through the mean percentage error (*MPE*), defined by the formula:

$$MPE\,Q_{sim} = \frac{100}{N}\sum_{j=1}^{N}\frac{|Q_{sim,j} - Q_{obs,j}|}{Q_{obs,j}} \tag{20}$$

where Q_{sim} coincides with Q_{sim1} or Q_{sim2} depending on the case considered.

The mean percentage error *MPE* Q_{sim} for all the considered cross-sections, as shown in Table 2, ranges between 0 and 5% for Q_{sim1} and 0 and 2% per Q_{sim2} (corresponding to R2 equal to 0.992 and 0.995, respectively). In light of this result, both Equations (17) and (19) can be deemed particularly reliable in discharge estimation when a good dataset, consisting of several velocity measurements over the whole flow area, is available.

Table 2 | *MPE* Q_{sim} of the discharges Q_{sim1} and Q_{sim2} obtained from the set of velocity data S1 for the cross-sections examined

	Set S1	
	***MPE* Q_{sim1} [%]**	***MPE* Q_{sim2} [%]**
Ponte Nuovo	4.80	2.36
Santa Lucia	3.64	3.56
Pontelagoscuro	5.18	3.84
Ohio	0.27	0.14
Allegheny	0.18	1.61
Monongahela	1.86	2.29

It should be noted that in the case of the Ohio, Allegheny and Monongahela river cross-sections, for which velocity measurements of only one flood event were available, the value of *MPE* Q_{sim} corresponds to the percentage error committed in estimating the discharge of this event alone on the transect considered.

Second step

As previously noted, the simulated discharges Q_{sim1} and Q_{sim2}, despite being derived using different formulations, were both based on the whole number of discharge values corresponding to the number of point velocity measurements considered simultaneously. In this second step, an analysis was conducted to assess sensitivity to the position of the velocity measurement used to estimate discharge; for this purpose, it was necessary to focus our attention on a single event, which in the cases of Ponte Nuovo, Santa Lucia, Pontelagoscuro corresponds to the most severe event, whereas in the case of the Ohio, Allegheny and Monongahela cross-sections it coincides with the only available event. With respect to the observed discharges for the events selected, indicated as Q_{obs}, Figure 8 shows the spatial distribution of the error in the discharge estimate $(|Q_i - Q_{obs}|/Q_{obs}) \times 100$ with $i = 1,2.. n_{meas}$, obtained downstream of the two-dimensional mapping of errors associated with the available measurement points, limited to the sampled area where both devices, current meter or ADCP instrumentation, were able to measure velocity. Therefore, in Figure 8, blank zones near the bottom and banks refer to the unsampled portions of the flow area.

As may be seen from Figure 8, in all cases studied, the points nearest the bottom and banks generally lead to larger errors, whereas points in the central/upper part of the flow area enable a more accurate estimation. This tends to be the case, first, because in the bottom part of the cross-section the observed values associated with the isovels are lower; thus a minor error in the velocity

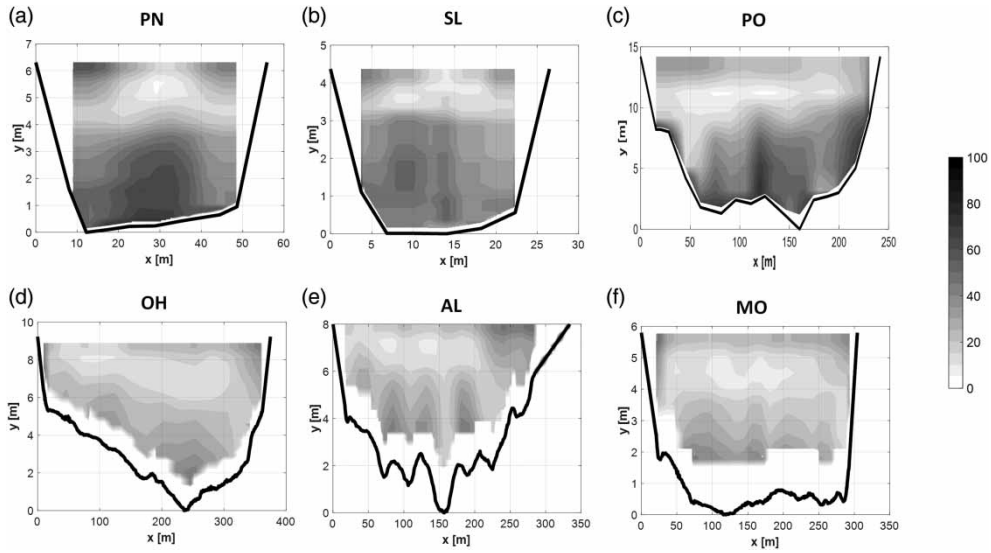

Figure 8 | Spatial distribution of the error committed in the estimation of discharge according to the position of the velocity measurement used to calculate the cross-sectional mean velocity in the analysed river sites: (a) Ponte Nuovo (PN), (b) Santa Lucia (SL), (c) Pontelagoscuro (PO), (d) Ohio (OH), (e) Allegheny (AL), (f) Monongahela (MO). Blank areas near the bottom and banks refer to the unsampled zone where the device (current meter or ADCP) could not measure velocity.

measurement can cause a large error in the estimate of discharge. In other words, the calculation of the mean velocity, obtained through the ratio between the measured velocity u and the associated dimensionless value η of Equation (15), is more sensitive to the precision of the measurements when they are based on small values of η, i.e., in proximity to the wetted perimeter. Second, it is also possible that the velocity point position is incorrectly evaluated and thus associated with a wrong value of η, due to the high velocity gradient which typically characterized the portion of the flow area close to the contour.

In light of these results, the calculation of discharge was repeated for all the cases studied considering a portion of the n_{meas} velocity measurements, preferentially those corresponding to points positioned in the upper/central part of the cross-section. This would in any case enable an accurate estimate of discharge to be obtained, while also serving to reduce both the time and cost of velocity sampling procedures.

Discharge was calculated using the specific selections/set of measurements shown in Figure 9 with reference to a generic section, where the *y-axis* indicates the vertical corresponding to the maximum surface velocity, H the depth along the *y-axis*, L the flow width and S1 the complete set of n_{meas} velocity measurements:

- S2: portion of the measurements of S1 positioned within the rectangular area centred in relation to the *y-axis* and having dimensions of $L/2$ and $H/2$;
- S3: the measurements taken starting from the free surface along the *y-axis* until reaching a depth equal to $H/2$;
- S4: the maximum surface velocity u_D alone.

As can be seen from Figure 9, these sets of measurements lead to a substantial reduction in the sampling phase. It is worth noting that, even if set S4 consists of the maximum surface velocity only, operatively it still requires the sampling of some velocity points in the central portion of the flow width in order to properly identify the maximum surface velocity. This operation can be easily performed through a radar gun, for instance.

Table 3 shows for each case study and for each set of velocity data the range (over the whole number of events considered) of measurements n_{meas} used; in particular, for the Ohio, Allegheny and Monongahela river cross-sections, just one value for each set of velocity is provided there being only one event available for each section.

Figure 10 shows the *MPE* Q_{sim} we obtained on the basis of the N pairs of values $Q_{sim1} - Q_{obs}$ (Figure 10(a)) and $Q_{sim2} - Q_{obs}$ (Figure 10(b)) upon varying the sets of point

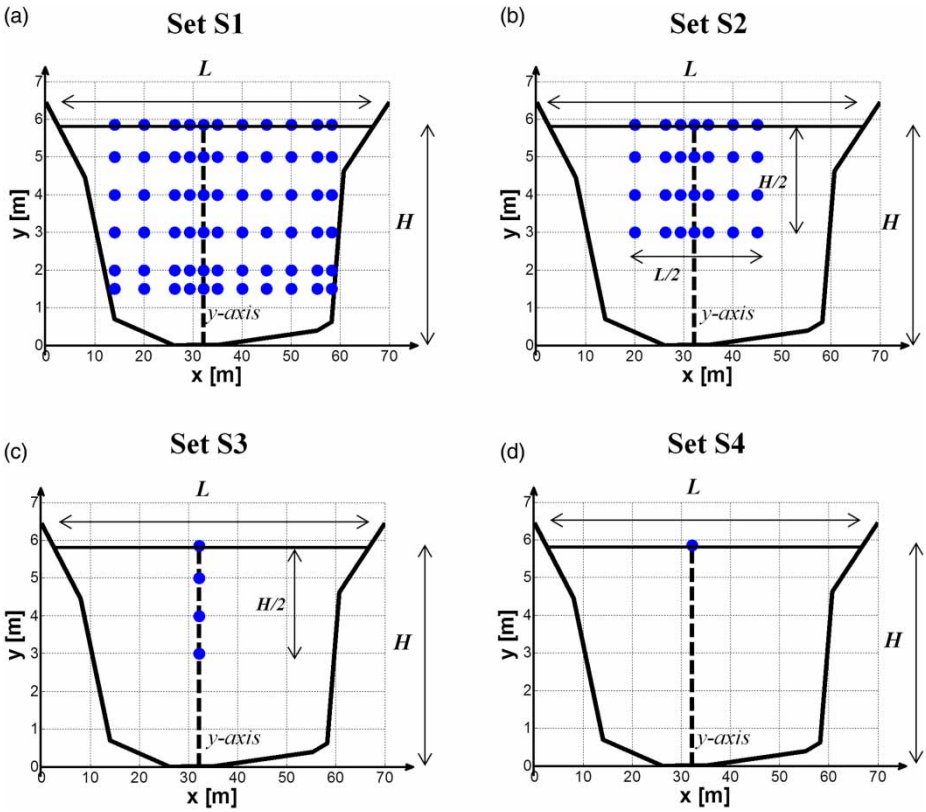

Figure 9 | Set of velocity measurements used to calculate the discharges Q_{sim1} and Q_{sim2} in a generic section: (a) set S1, (b) set S2, (c) set S3, (d) set S4.

Table 3 | Range of the number of measurements n_{meas} (over the whole set of events considered) for each set of velocity data at river gauging stations

	n_{meas}			
	Set S1	**Set S2**	**Set S3**	**Set S4**
Ponte Nuovo	39–97	10–34	3–6	1
Santa Lucia	19–62	9–21	3–5	1
Pontelagoscuro	76–115	17–42	3–7	1
Ohio	6,449	3,088	9	1
Allegheny	2,217	1,218	7	1
Monongahela	2,481	860	5	1

velocity measurements listed above for the different cross-sections considered, all assumed to have a uniform roughness distribution.

A striking similarity can be observed between Figure 10(a) and 10(b). This demonstrates that the two formulations proposed for the estimation of discharge can be considered equivalent, irrespective of the number of velocity measurements used. In particular, *MPE* Q_{sim1} is equal to *MPE* Q_{sim2} where set S4 was used. It is, in fact, evident that the formulations of Equations (17) and (19) will provide the same value of discharge ($Q_{sim1} = Q_{sim2}$) if associated with set S4, since given that the surface maximum velocity u_D is the only point measurement available, the simulated discharge will correspond to the discharge $(u_D/\eta(u_D))A$, irrespective of which formulation is chosen.

Irrespective of the method used to estimate discharge (Q_{sim1} or Q_{sim2}), the selection of S2 and S3 leads to ranges of *MPE* Q_{sim} that are slightly greater than those obtained with set S1, with values of *MPE* Q_{sim} ranging from 2 to 13% in the case of S2 and from 4 to 14% in the case of S3. Finally, it is worth observing that S4, despite relying on a single velocity measurement, nonetheless enables a reliable estimate of discharge to be obtained, as *MPE* Q_{sim} is always kept within 10%.

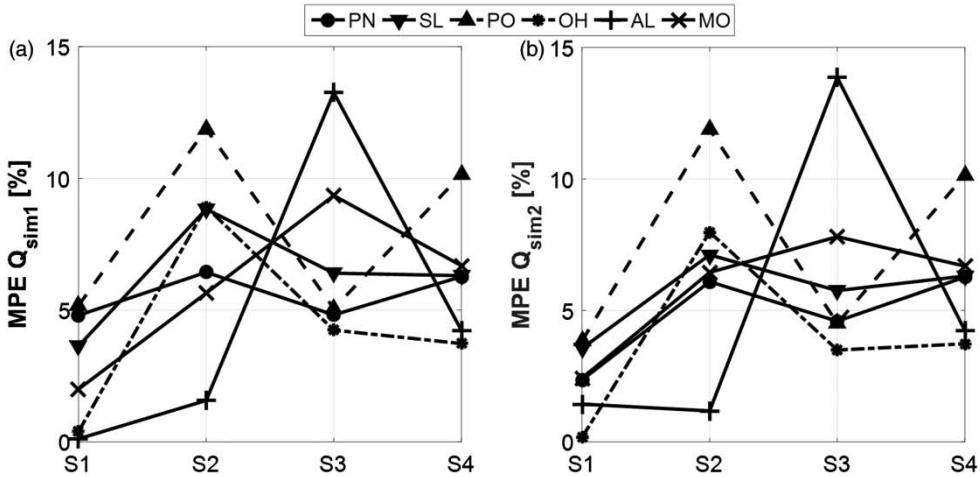

Figure 10 | Trend in the *MPE* Q_{sim} of the discharges Q_{sim1} (a) and Q_{sim2} (b) according to the set of velocity data for the cross-sections examined used in the estimation: Ponte Nuovo (PN), Santa Lucia (SL), Pontelagoscuro (PO), Ohio (OH), Allegheny (AL), Monongahela (MO).

Such an analysis, while confirming a general trend for the *MPE* Q_{sim} which overall grows passing from S1 to S4, it also highlights a clear variability both for a given gauge section and, for a given set, considering the different sections. This is mainly due to the dispersion of the velocity measurements which is extremely high particularly during important flood events. In fact, velocity measurements are difficult to perform at increasing depth, while velocity measurements near the surface or at the surface in the central part of the cross-section are easier and thus less affected by errors. This stresses the importance of the result relating to S4, where even though a single measurement is considered, the approximation in discharge estimate is limited.

Furthermore, it is worth noting that the results obtained with S4 (*MPE* $Q_{sim} < 10\%$) are comparable to the ones gained by applying the entropy concept, coupled with a method for determining the entropy parameter M based on the knowledge of the cross-section geometry and the only maximum surface velocity measurement (Farina *et al.* 2014). Indeed, for the PN case study, in Farina *et al.* (2014), a *MPE* Q_{sim} around 10% was obtained by using the only maximum surface velocity measurement, which is comparable with, and even slightly higher than, the one obtained with the proposed method, which is around 7% (see Figure 10).

CONCLUSIONS

This paper proposes a method for estimating discharge in a channel cross-section which is based on the application of the Biot–Savart law and aims to quantify the effect produced on velocity at a generic point of the cross-section by the generic portions into which the wetted perimeter is divided. Unlike Maghrebi's approach, the method proposed enables us to reconstruct the isovel pattern within the cross-section taking into account the geometry of the bathymetric profile and the hydraulic roughness characteristics of the river bed according to Manning's coefficient embedded in the Chen power law.

After reconstructing the isovel pattern, the proposed method allows estimation of the mean velocity and hence discharge, by relying on at least one velocity measurement in that cross-section. In particular, for cases in which a number of velocity measurements are available for the cross-section in question, two different and novel formulations for estimating discharge have been proposed.

The proposed procedure is shown to reproduce the pattern of the isovels in a quite satisfying way and hence to estimate discharge through a limited number of velocity measurements. This was validated on the basis of numerous field velocity measurements made at various gauging stations: Ponte Nuovo and Santa Lucia (Tiber River), Pontelagoscuro (Po River), as well as several sites along the Ohio, Allegheny and Monongahela Rivers in the USA.

On the whole, both formulations for estimating discharge provide a good estimate in cases where their application relies on different measurements across the entire flow area. However, it has also been shown that measurements should be concentrated in the central/upper part of the cross-section in order to obtain reliable estimate of discharge. In particular, only measurement of the maximum surface velocity allows for estimate of discharge with a mean percentage error around or lower than 10%.

It is clear that a considerable advantage can be derived from using the method coupled with set S4 (a single surface velocity measurement) for the purpose of monitoring discharge. First of all, it enables the sampling procedure to be limited to an enormous degree, avoiding measurements at different depths that may be affected by errors which tend to increase with depth, as shown by the numerical example, and thus can undoubtedly save time and money. Moreover, the measurement is taken on the surface, and need not be made by an operator wading across the channel, as various techniques for measuring surface velocity are available today, including moving or fixed non-contact radar sensors and satellite data. These eliminate potential problems of exposing personnel to performing measurements in water with dangerously strong currents and thus they ensure maximum safety.

ACKNOWLEDGEMENTS

The authors wish to thank the Region of Umbria, Department of Environment, Planning and Infrastructure, and the US Geological Survey, WRD, Denver Federal Center, for providing Italian and American river basin data, respectively.

REFERENCES

Adrian, R. J. 1991 Particle-imaging techniques for experimental fluid-mechanics. *Annual Review of Fluid Mechanics* **23**, 261–304.

Biot, J. B. & Savart, F. 1820 Note sur le Magnétisme de la pile de Volta. *Annales de Chimieet de Physique* **15**, 222–223.

Bjerklie, D. M., Dingman, S. L., Vorosmarty, J. C., Bolster, C. H. & Congalton, R. G. 2003 Evaluating the potential for measuring river discharge from space. *Journal of Hydraulic Engineering* **278** (1–4), 17–38.

Chen, C. L. 1991a *Power-law of Flow Resistance in Open Channel: Manning Formula Revisited*. Centennial of Manning's Formula, Water Research, Charlottesville, VA, pp. 206–240.

Chen, C. L. 1991b Unified theory on power laws for flow resistance. *Journal of Hydraulic Engineering* **117** (3), 371–389.

Cheng, R. T., Gartner, J. W., Mason, R. R., Costa, J. E., Plant, W. J., Spicer, K. R., Haeni, F. P., Melcher, N. B., Keller, W. C. & Hayes, K. 2004 *Evaluating a Radar-Based, Non-Contact Streamflow Measurement System in the San Joaquin River at Vernalis, California*. US Geological Survey, Menlo Park, CA.

Chiu, C. L. 1987 Entropy and probability concepts in hydraulics. *Journal of Hydraulic Engineering* **113** (5), 583–600.

Chiu, C. L. 1988 Entropy and 2-D velocity in open channels. *Journal of Hydraulic Engineering* **114** (7), 738–756.

Chiu, C. L. 1989 Velocity distribution in open channels. *Journal of Hydraulic Engineering* **115** (5), 576–594.

Chiu, C. L. 1991 Application of entropy concept in open channel flow study. *Journal of Hydraulic Engineering* **117** (5), 615–628.

Chiu, C. L. & Abidin Said, C. A. 1995 Maximum and mean velocities and entropy in open-channel flow. *Journal of Hydraulic Engineering* **121** (1), 26–35.

Chiu, C. L. & Chiou, J. D. 1986 Structure of 3-D flow in rectangular open channels. *Journal of Hydraulic Engineering* **112** (11), 1050–1067.

Chiu, C. L. & Murray, D. W. 1992 Variation of velocity distribution along non-uniform open-channel flow. *Journal of Hydraulic Engineering* **118** (7), 989–1001.

Chiu, C. L. & Tung, N. 2002 Maximum velocity and regularities in open-channel flow. *Journal of Hydraulic Engineering* **128**, 390–398.

Chow, V. T. 1959 *Open-Channel Hydraulics*. McGraw-Hill, New York.

Corato, G., Melone, F., Moramarco, T. & Singh, V. 2012 Uncertainty analysis of flow velocity estimation by a simplified entropy model. *Hydrological Processes* **28** (3), 581–590.

Costa, J. E., Spicer, K. R., Cheng, R. T., Haeni, F. P., Melcher, N. B. & Thurman, E. M. 2000 Measuring stream discharge by noncontact methods: a proof-of-concept experiment. *Geophysical Research Letters* **27**, 553–556.

Costa, J. E., Cheng, R. T., Haeni, F. P., Melcher, N., Spicer, K. R., Hayes, E., Plant, W., Hayes, K., Teague, C. & Barrick, D. 2006 Use of radars to monitor stream discharge by noncontact methods. *Water Resources Research* **42**, W07422.

Creutin, J. D., Muste, M., Bradley, A. A., Kim, S. C. & Kruger, A. 2003 River gauging using PIV techniques: a proof of concept experiment on the Iowa River. *Journal of Hydrology* **277**, 182–194.

Farina, G., Alvisi, S., Franchini, M. & Moramarco, T. 2014 Three methods for estimating the entropy parameter M based on a decreasing number of velocity measurements in a river cross-section. *Entropy in Hydrology* **16** (5), 2512–2529.

Fulton, J. & Ostrowski, J. 2008 Measuring real-time streamflow using emerging technologies: radar, hydroacoustics, and the probability concept. *Journal of Hydrology* **357**, 1–10.

Halliday, D. & Resnick, R. 1990 *Fundamentals of Physics*. John Wiley & Sons, Hoboken, NJ.

Hayt, W. H. 1981 *Engineering Electromagnetics*, 4th edn. McGraw-Hill, New York.

Herschy, R. W. 2009 *Streamflow Measurement*, Taylor and Francis, Boca Raton, FL.

Jaynes, E. T. 1957 Information theory and statistical mechanics. I. *Physical Review* **106**, 620–630.

Jodeau, M., Hauet, A., Paquier, A., Le Coz, J. & Dramais, G. 2008 Application and evaluation of LS-PIV technique for the monitoring of river surface velocities in high flow conditions. *Flow Measurement and Instrumentation* **19**, 117–127.

Krishnappan, B. G. & Lau, Y. L. 1986 Turbulence modeling of flood plain flow. *Journal of Hydraulic Engineering* **112** (4), 251–266.

Lee, M. C., Lai, C. J., Leu, J. M., Plant, W. J., Keller, W. C. & Hayes, K. 2002 Noncontact flood discharge measurements using an X-band pulse radar (I) theory. *Flow Measurement and Instrumentation* **13**, 265–270.

Maghrebi, M. F. 2003 Discharge estimation in flumes using a new technique for the production of isovel contours. In *Proceedings of International Conference on Civil and Environment Engineering, ICCEE*, pp. 147–156.

Maghrebi, M. F. 2006 Application of the single point measurement in discharge estimation. *Advances in Water Resources* **29** (10), 1504–1514.

Maghrebi, M. F. & Rahimpour, M. 2005 A simple model for estimation of dimensionless isovel contours in open channels. *Flow Measurement and Instrumentation* **16** (6), 347–352.

Marchi, E. & Rubatta, A. 1981 *Meccanica dei Fluidi. Principi ed Applicazioni (Fluid Mechanics. Principles and Applications)*. UTET, Torino.

Melcher, N. B., Costa, J. E., Haeni, F. P., Cheng, R. T., Thurman, E. M., Buursink, M., Spicer, K. R. & Hayes, E. 2002 River discharge measurements by using helicopter-mounted radar. *Geophysical Research Letters* **29**, 41-1–41-4.

Moisello, U. 1998 *Idrologia tecnica [Technical Hydrology]*. La Goliardica Pavese, Pavia, p. 824 (in Italian).

Moramarco, T. & Singh, V. 2010 Formulation of the entropy parameter based on hydraulic and geometric characteristics of river cross sections. *Journal of Hydrologic Engineering* **15** (10), 852–858.

Moramarco, T., Saltalippi, C. & Singh, V. 2004 Estimation of mean velocity in natural channels based on Chiu's velocity distribution equation. *Journal of Hydrologic Engineering* **9** (1), 42–50.

Nezu, I. & Nakagawa, H. 1993 *Turbulence in Open-Channel Flows*. A. A. Balkema, Rotterdam.

Rahimpour, M. & Maghrebi, M. F. 2006 Prediction of stage–discharge curves in open-channels using a fixed-point velocity measurement. *Flow Measurement and Instrumentation* **17** (5), 276–281.

Rantz, S. E. 1982 *Measurement and Computation of Streamflow. Volume 1: Measurement of Stage and Discharge*. US Geological Survey Water Supply Paper 2175.

RDI 2007 *WinRiver II: User's Guide*. Teledyne RD Instruments, Poway, CA.

Rodi, W. 1993 *Turbulence Models and their Application in Hydraulics*. A. A. Balkema, Rotterdam.

Rouse, H. 1950 *Engineering Hydraulics*. Wiley, New York.

Strickler, A. 1923 BeitragezurFrage der Geschwindigkeitsformel und der Rauhigkeitszahlen fur Strome, Kanale und geschlosseneLeitungen, Mitteilungen des eidgenossischenAmtes fur Wasserwirtschaft, Bern, Switzerland, No. 16 (Translated as 'Contributions to the question of a velocity formula and roughness data for streams, channels and closed pipelines' by T. Roesgan and W. R. Brownie, Translation T-10, W. M. Keck Laboratory of Hydraulics and Water Resources, California Institute of Technology, Pasadena, CA. January 1981).

Tauro, F., Grimaldi, S., Petroselli, A. & Porfiri, M. 2012 Fluorescent particle tracers for surface flow measurements: a proof of concept in a natural stream. *Water Resources Research* **48**, W06528.

Tauro, F., Pagano, C., Phamduy, P., Grimaldi, S. & Porfiri, M. 2015 Large-scale particle image velocimetry from an unmanned aerial vehicle. *IEEE/ASME Transactions on Mechatronics* **20**, 3269–3275.

Tauro, F., Olivieri, G., Petroselli, A., Porfiri, M. & Grimaldi, S. 2016 Flow monitoring with a camera: a case study on a flood event in the Tiber River. *Environmental Monitoring and Assessment* **188**, 118.

UNI EN ISO 748 2008 *Hydrometry, Measurement of Liquid Flow in Open Channels Using Current-Meters or Floats*. International Organization for Standardization.

Wright, S. & Parker, G. 2004 Flow resistance and suspended load in sandbed rivers: simplified stratification model. *Journal of Hydraulic Engineering* **130** (8), 796–805.

Xia, R. 1997 Relation between mean and maximum velocities in a natural river. *Journal of Hydraulic Engineering* **123** (8), 720–723.

Yamaguchi, T. & Niizato, K. 1994 Flood discharge observation using radio current meter. *Doboku Gakkai Rombun-Hokokushu Proceedings of the Japan Society of Civil Engineers* **497**, 41–50.

Yen, B. C. 2002 Open channel flow resistance. *Journal of Hydraulic Engineering* **128** (1), 20–39.

First received 13 January 2016; accepted in revised form 13 February 2017. Available online 5 April 2017